مجلة جامعة بني وليد للعلوم الإنسانية والتطبيقية

تصدر عن جامعة بني وليد – ليبيا

Website: https://jhas-bwu.com/index.php/bwjhas/index

العدد التاسع والعشرون، 2023

A comparative study on soil stabilisation with calcium and magnesium-based binders.

M. Ebailila[1*], J. Kinuthia[2], J. Oti[3], A. Muhmed[4],
[1]Department of Civil Engineering/Faculty of Engineering/ Bani Waleed University, Libya
[2,3] Faculty of Computing, Engineering and Science/University of South Wales, UK
[4] Department of Civil Engineering/Faculty of Engineering/Tobruk University, Libya
*Crosspnding author: mansour.ebailila@yahh.co.uk

تاريخ الاستلام: 2023-06-14 تاريخ القبول: 2023-06-30 تاريخ النشر : 2023-09-07

Abstract: Soil stabilisation using cementitious materials is a promising technique for improving the mechanical characteristics and suppressing the swelling of expansive and sulfate soil. This study compares the viability of two calcium-based stabilisers (Portland cement-C and lime-L) and one MgO-based stabiliser (magnesium oxide-M) in soil stabilisation. A set of specimens produced by use of two soil materials (pure kaolin soil and artificially gypsum-dosed kaolin) at a constant stabiliser content of 10 wt%, were examined in terms of the unconfined compressive strength (UCS), swelling and derivative thermogravimetric (DTG) analysis. Accordingly, the results revealed that Portland cement (10%C) experienced a superior UCS of 1830 kN/m^2 and expansion of 0.44% in the absence of sulfate, whereas magnesium oxide (10%M) outperformed both Portland cement and lime in the suppression of swelling of the artificial sulfate soil, where it induced an expansion magnitude of 1%, relative to that of 15% and 24% for 10%C and 10%L, respectively. However, the 10%M yielded a lower UCS (927 kN/m^2) relative to that of 2030 kN/m^2 for 10%C and 1995 kN/m^2 for 10%L in the presence of sulfate. The superiority of 10%C in the absence of sulfate is due to its higher Si^{+4} and Al^{+3} ions, which provide the needed oxides for the nucleation of the hydrates that interlock the system. As for the dominance of 10%M in the suppression of expansion of sulfate kaolin, it can be assigned to the restriction of the nucleation and growth of ettringite crystals owing to the unavailability of calcium ions.

Keywords: (Ettringite, Portland cement, lime, magnesium oxide, linear expansion, swelling)

Introduction

Expansive soil materials, which are distributed worldwide, is normally characterized as problematic soil due to its sensitivity to change under moisture fluctuation [1], thus inducing shrink-swell behaviour [2]. This reversible shrink-swell behaviour represents a challenging task and threatens sustainability [3], by inducing differential settlement, crack formation, and overlying structure collapse [4]. Therefore, the construction of engineering structures such as pavements and highway embarkments on such soil can be destructive [5], due to its unpredictable behaviour.

To suppress the reversible shrink-swell behaviour of the expansive soil, engineers traditionally tend to treat the available soil with cementitious materials such as calcium-based stabiliser (Portland cement and lime) due to their efficiencies in enhancing the physicomechanical properties such as the reduction of plasticity, swelling and permeability, as well as increase of shear strength, UCS, bearing capacity and durability resistance [5-8]. However, there have been some environmental concerns related to the manufacturing of calcium-based stabilisers such as the higher energy consumption (5000 MJ/t for cement and 4000 MJ/t for lime) associated with their production, with a carbon dioxide emission of 1000 and 800 kg/ton, respectively [6]. Calcium-based stabilisers also exhibit a limited efficiency in the treatment of sulfate-bearing soils due to the formation of ettringite (see equation 1) from the interaction between calcium, alumina (from soil), sulfate (from soil or groundwater), and water [7].

$$6Ca^{2+} + 2Al(OH)_4^- + 4OH^- + 3(SO_4)^{2-} + 26H_2O \rightarrow Ca_6[Al(OH)_6]_2 \cdot (SO_4)_3 \cdot 26H_2O \text{ ....}(1)$$

Correspondingly, engineering researchers have investigated several techniques including double application of lime, pre-compaction mellowing, pre-treatment with barium compounds, use of sulfate resistance cement and use of agricultural and industrial by-products, to improve the properties of expansive soil and preserve the economy [8].

Recently, reactive magnesia (MgO) is gaining great attention, particularly in sulfate-bearing soils. This is probably due to its higher surface area, its higher reactivity [9], lower manufacturing temperature (700-1000°C) [10-11], and lesser energy needs (2400 MJ/t) [12], although it induces a higher carbon dioxide emissions of 1.4 ton per ton [13], relative to 0.95 tons of CO_2 for cement and 0.8 ton of CO_2 for lime [9,14]. Of course, these carbon dioxide emissions are not promising and may form the refusal of its applications. Nevertheless, Liska and Al-Tabbaa [13] conducted a research study on MgO and reported that MgO can reach a 71% carbonation, suggesting the reduction of CO_2 from 1400 to 420 kg/tone.

Concerning the research studies on the effect of magnesium oxide (M), Seco et al., (2011) [15] carried out a comparative study between magnesium oxide and other pozzolans (including coal bottom ash, rice husk ash, steel fly ash and lime among others) in the stabilisation of expansive soil. The results revealed a superior swelling performance in the case of magnesium oxide at a binder dosage of 2%, while lime induced a lower swelling magnitude at a binder content of 4%. Li et al., (2019) [11] investigated the efficiency of lime, Portland cement, and magnesium oxide on the stabilisation/solidification of heavy metals-contaminated soils and concluded that no single binder can be effective for all the heavy metals, thus the choice of binder is a site-specific problem. Li et al., (2020) [16] compare MgO-activated ground granulated blast-furnace slag (MgO-GGBS) with cement on the swelling suppression of sulfate soil and observed a better swelling behaviour and superior residual strength after soaking in water for the case of MgO-activated GGBS, which was in line with [9,12,17-24]. So far, however, there is a lack of comparative studies between quicklime, Portland cement and magnesium oxide on the stabilisation of both non-sulfate and sulfate-bearing soil.

To this end, the key aim of this research was to determine the optimum binder (among Portland cement, lime, and magnesium oxide) in terms of both UCS and expansion kaolin soil in the presence and absence of gypsum.

Methodology

1- Materials

The raw materials used in this study included kaolin soil (K), gypsum (G), Portland cement (PC), lime (L) and magnesium oxide (M). **Table 1** and **Table 2** outline the oxide and physical characteristics of the raw materials, respectively, whereas **Fig.1** plots the results of sieve analysis for the raw materials.

Table 1: Oxide compositions of kaolin, Portland cement, lime, and magnesium oxide.

Oxides	K	C	L	M
CaO	0.01	61.5	71.6	-
MgO	0.21	3.54	0.58	>98
SiO_2	47.3	18.8	0.67	-
Al_2O_3	35.9	4.77	0.07	-
Na_2O	0.07	0.02	0.02	-
P_2O_5	0.01	0.1	0.03	-
Fe_2O_3	0.7	2.87	0.05	-
Mn_2O_3	0.02	0.05	0.02	-
K_2O	1.79	0.57	0.01	-
TiO_2	0.02	0.26	0.01	-
V_2O_5	0.01	0.06	0.02	-
BaO	0.07	0.05	0.01	-
SO_3	0.01	3.12	0.19	-
LOI	0.1	4.3	27.4	-

Table 2: Some physical characteristics of kaolin, Portland cement, lime, magnesium oxide.

Properties	K	C	L	M
Bulk density (kg/m^3)	-	1400	480	-
Specific gravity (Mg/m^3)	2.14	3.15	2.82	3.58
pH Value	5.37	13.41	12.62	11.90
Colour	White	Grey	White	White

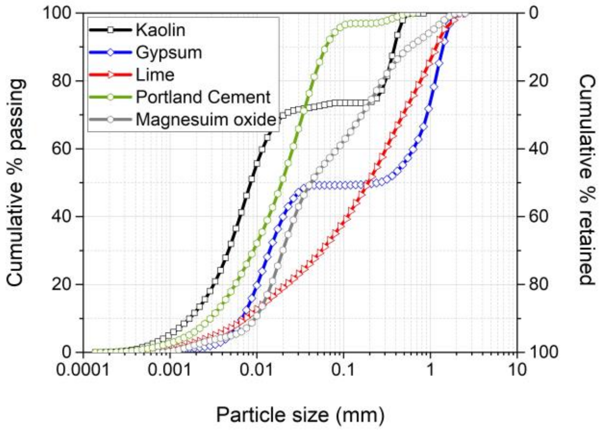

Fig.1: Sieve analysis results of kaolin, gypsum, lime, Portland cement and magnesium oxide.

The kaolin (K) used was an industrial kaolin soil, sourced from Potterycrafts Ltd, Stoke-on-Trent, UK. It has a liquid limit, plastic limit, and plasticity index of 56.7%, 33.3%, and 23.4%, respectively. Therefore, the kaolin was characterized as a medium-graded sandy SILT.

The gypsum (G) used was a calcium sulfate dihydrate and has a physical form of white powder; it was obtained from Fisher Scientific Ltd, Loughborough, Leicestershire, UK. The gypsum was used to prepare an artificial gypsum-bearing soil, based on the premise of being the most typical source of sulfate type encountered in natural sulfate-bearing soils.

The cement (C) used was a commercially available CEM-I Portland cement having grey colour; it was produced in line with BS EN 197-1: 2011 [25], and supplied by Large Cement, UK. The utilization of this type of cement in this study can be credited to its traditional recognition in the treatment of clay soils.

The lime (L) used was in the form of off-white quicklime with a relative density of 3.31: it was sourced from Tarmac Cement and Lime Company, Derbyshire, Derby, UK. The choice of adopting quicklime in this study is attributed to its relatively higher calcium content, facilitating the faster drying of moisture content within soil and in turn enables the best degree of soil stabilisation [26-29].

The magnesium oxide (M) used was a commercial reactive magnesia having a physical form white powder; it was obtained from Fisher Scientific Ltd, Loughborough, Leicestershire, UK.

2- Mix proportions

The mix configurations (see **Table 3**) evaluated in the laboratory experimentations involved using; 1) two soil materials including pure kaolin soil and gypseous kaolin soil); 2) three different binders (Portland cement, lime, and magnesium oxide); and 3) fixed moisture content of 31%.

Table 3: Mix compositions of designed soil mixes stabilised with different binders.

Design code	Target soil materials (%)		MC	Binder in % by target soil material		
	K	G		L	C	M
K0G-10%L	100	0	31	10		
K0G-10%C	100	0	31		10	
K0G-10%M	100	0	31			10
K9G-10%L	91	9	31	10		
K9G-10%C	91	9	31		10	
K9G-10%M	91	9	31			10

For clarity, the mix design code comprised of kaolin (K), gypsum (G) and the binder (C for Portland cement, L for lime or M for magnesium oxide), of which G, C, L and M proceeded by a number, representing the solid amount. The gypsum content displayed in the design code denotes the gypsum percentage by the total mass of gypseous kaolin, while the stabilizer amount represents the stabilizer dosage by the total mass of dry soil materials.

The gypseous kaolin was prepared by blending kaolin soil with 9 wt% of gypsum in a dry form. The choice of adopting pure kaolin and gypseous-bearing kaolin soil was due to; 1) the homogeneity of kaolin soil, as it simplifies the understanding of the interactions; 2) the relatively higher alumina content of kaolin, as it enables the nucleation of relatively higher ettringite quantity; 3) the gypsum is the commonly encountered source of sulfate in natural sulfate soil; and 4) the gypsum content of 9%, was the worst sulfate concentration for ettringite nucleation [6,8,14,30]. The purpose of using three binders was to select the optimum binder in the presence and absence of sulfate. As for the adoption of 31 % moisture content, which was equal to 1.1 of the corresponding standard proctor optimum condition, it was because the soil is always compacted wet of moisture to actualize the best durability performance [6,8,14,30]. In addition, it was not found necessary to establish the optimum moisture content (OMC) for each system due to the time-consuming nature of proctor test and the impracticability of establishing the OMC for each mix [30].

3- Specimen preparation

A total of 11 stabilized samples were produced for each mix. Two of these samples were used for simulating the swelling behaviour, whereas nine samples were used for evaluating the UCS after 7, 28 and 90 days of moist curing. For each specimen, adequate quantity of dry materials, as per the mix composition outlined in **Table 3**, capable of manufacturing stabilised sample with dimensions of 50 mm in diameter and 100 mm in height, were blended in dry form using a mixer for 3 minutes. Hereafter, the moisture content was added, and the mixing was continued for further three minutes to ensure the homogeneity of the mixture. Consequently, the semi-paste was accommodated into a steel mould and compacted by use of a jack in aid of a steel frame as detailed in [6]. At the end of three minutes for specimen stability, the stabilized sample was extruded by use of a plunger, wrapped in a cling film, and stored in a plastic container at 20 ± 2, allowing for moist curing.

4- Testing method

4.1- UCS

The UCS test was conducted, in line with BS EN ISO 17892-7: 2018 [31], on three samples per mix after each of the prescribed moist curing periods (7, 28 and 90 days). Three specimens were axially compressed using a Hounsfield Testing Machine (see **Fig.2**) at a displacement ratio of two mm per minute. The average of the UCS of three specimens was calculated and used as the representative UCS.

Fig.2: The 10kN capacity Hounsfield compression machine.

4.2- Swelling

The swelling behaviour (linear expansion) was conducted on two samples per mix composition, in accordance with BS EN 13286-49: 2004 [32], using Perspex cells (see **Fig.3**), as commonly adopted in the literature [6, 8, 14, 33–35].

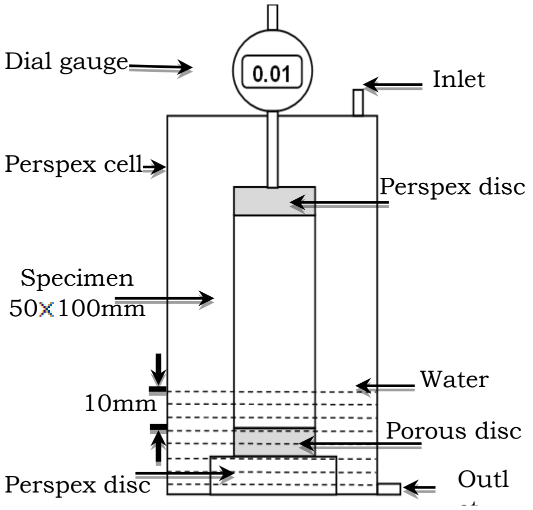

Fig.3: The Perspex cell set-up used for the vertical displacement (swelling) measurement.

Immediately, after seven days of moist curing, about ten mm of the upper and bottom part of the stabilized samples were unwrapped and accommodated separately in the Perspex cell as shown in **Fig.4**.

Fig.4: Linear expansion specimens under expansion measurement.

Afterwards, the dial gauge was adjusted to zero, and the water was added through the inlet until the bottom ten mm part of the samples was soaked in water, allowing for expansion. This water height was used for the reason that it was adopted in several publications [33–35]. Subsequently, the dial gauge reading was monitored periodically, and the ratio (%) of dial gauge reading (mm) to the original height (100 mm) of the specimens was calculated randomly through a prolonged water soaking period of 200 days. Finally, the mean vertical movement (linear expansion value) of the two stabilized samples was then calculated and represented as the linear expansion (swelling) magnitude of the mix.

4.3- Derivative thermogravimetric analysis

The derivative thermogravimetric (DTG) analysis was carried out from 20±5 ℃ up to 1000 ℃. The analysis was run at a heating ratio of 20 ℃/min and under an argon environment using a TGA55 kit shown in **Fig.5**. The specimen used for the analysis was taken from the fractured 7-day UCS specimens and after being dried with the aid of silica gel in a desiccator at a temperature of 40 ℃, in order to prevent hydration.

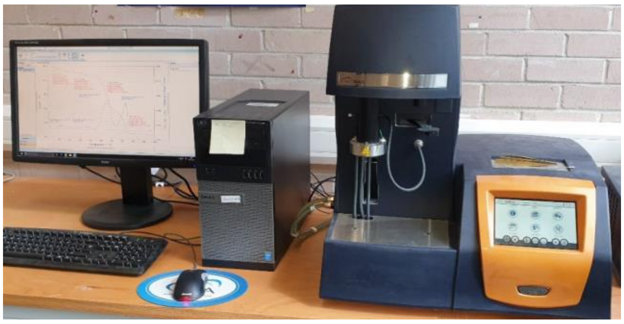

Fig.5: Thermogravimetric (TG) and derivative thermogravimetric (DTG) analyser used in this study (TGA55).

Results and discussion

1- UCS performance

Fig.6 illustrates the UCS evolution over a moist curing period of up to 90 days for pure and gypseous kaolin soil stabilized with 10%C, 10%L, and 10%M.

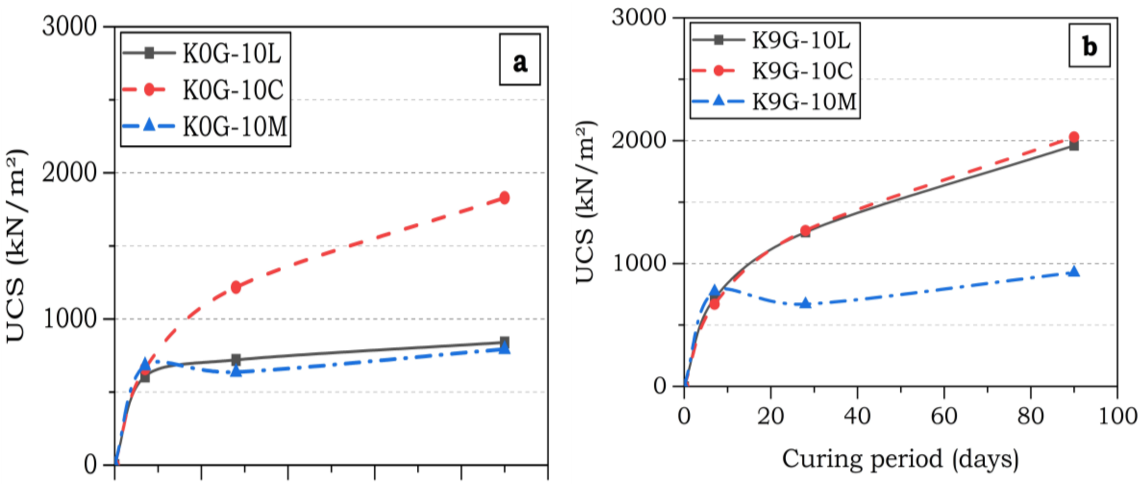

Fig.6: The UCS development of **a)** kaolin and **b)** gypseous kaolin specimens, made with lime, Portland cement and magnesium oxide.

In general, there was a gradually increasing strength trend over 90 days of moist curing, suggesting the continuous development of hydrates, and indicating that the samples followed the typical UCS trend of soil stabilization [6,8,14,33–35]. The display of strength development in a 10%C-based system is commonly assigned to cement hydration, which forms hydrates such as calcium silicate hydrate (C-S-H) and calcium aluminate hydrate (C-A-H). These hydrates crystalline with time and interlock the soil system [36]. As for the 10%L and 10%M-based systems, the UCS development is because of the cation exchange, flocculation, and agglomeration of soil particles) as well as the pozzolanic reactions [6,7,37]. These reactions, therefore, form a stiff matrix and increase the robustness against loading, thus increasing the strength performance [30].

In the non-attendance of gypsum, the result revealed that the stabiliser domination with respect to the highest UCS was in the order of 10%C>10%L>10%M, where the 90-day UCS was 1830, 839 and 793 kN/m^2, respectively. This, therefore, suggests the superiority of 10%C on the expense of 10%L and 10%M in the stabilization of non-sulfate soil. The possible explanation for the cement superiority is the higher amount of Si^{+4} and Al^{+3} ions of the cement-based system [38], which provide the needed oxides for the nucleation and growth of hydrated products that are responsible for strength evolution [39]. The presence of unconsumed portlandite in L-based and brucite in M-based system, as detected in the DTG curves (detailed later), is also a contributing factor to the superiority of cement, as these two minerals coat the soil particles, postponing the dissolution of soil minerals [40], delaying the pozzolanic reactions, and reducing the cohesion of the system [41]. In addition, the nucleation of ettringite in C-based system due to the reaction between gypsum, tricalcium aluminate and water is another contributing factor for the superiority of cement. The strength enhancement induced by the formation of ettringite occurs through; 1) the porosity reduction owing to the ettringite growth which fill the voids; 2) the dewatering of the system owing to higher water absorption of the ettringite; and 3) the interlocking of the system owing to the growth of ettringite crystals surrounding the soil particles [6,30,42,43]. As for the better UCS induced by lime relative to magnesium oxide, this could be assigned to the lower reactivity of the magnesium oxide which is known to be a contributor to the performance of the magnesium oxide-based system [8].

In the presence of gypsum (sulfate), the UCS observations revealed that across all the formulations, the UCS of gypseous kaolin also outperformed their counterparts of pure kaolin at all the curing ages, and such superior performance, was more pronounced in specimens stabilized with calcium-based stabilizer (L and C). In this context, the stabilizer domination was in the sequential order of 10%C>10%L>10%M, where 10%C experienced the highest 90-day UCS of 2030 kN/m^2, relative to that of 1995 kN/m^2 for 10%L and 927 kN/m^2 for 10%M. With further in-depth, however, it can be inferred that the positive effect of sulfate was not consistent across all the formations, where lime-based specimens experienced the greatest UCS gain of 1156 kN/m^2, representing a strength gain ratio of about 140% relative to its stabilized none-sulfate counterpart, whereas 10%C- and 10%M-based specimens yielded a UCS gain of 200 and 130 kN/m^2, accounting for a strength gain ratio of about 11% and 16% relative to their stabilized none-sulfate counterparts, respectively. To the best experience of the authors, the strength gain induced by the presence of sulfate in specimens stabilized with calcium-based stabilizer is because of the variation in the quantity of formed ettringite, which depends on the amount of lime, sulfate, alumina, and water of the system [14]. As for the slight strength gain of M-based specimen in the presence of sulfate, this could be accredited to the proper particle distribution and the introduction of calcium ions (from gypsum), of which the latter is expected to induce fabric modification due to cation exchange [8].

2- Linear expansion

Fig.7 displays the average linear expansion plots over a prolonged water soaking period of 200 days for kaolin samples stabilised with a single binder of 10%C, 10%L and 10%M. Like the case of UCS, the specimen stabilized with cement (K9G-10%C) exhibited the best (lowest) expansion magnitude of 0.44%, followed by K0G-10%M and K0G-10%L with an expansion magnitude of 0.66% and 4%, respectively. The reduction induced by C, L or M is already described in previous publications as a result of two reaction mechanisms; 1) fabric modification due to cation exchange, and flocculation and agglomeration of soil particles; and 2) the nucleation and growth of hydrates such as C-S-H, C-A-H, and M-S-H due to the pozzolanic reactions between the soil and the cementitious materials [7,8,14,44–48].

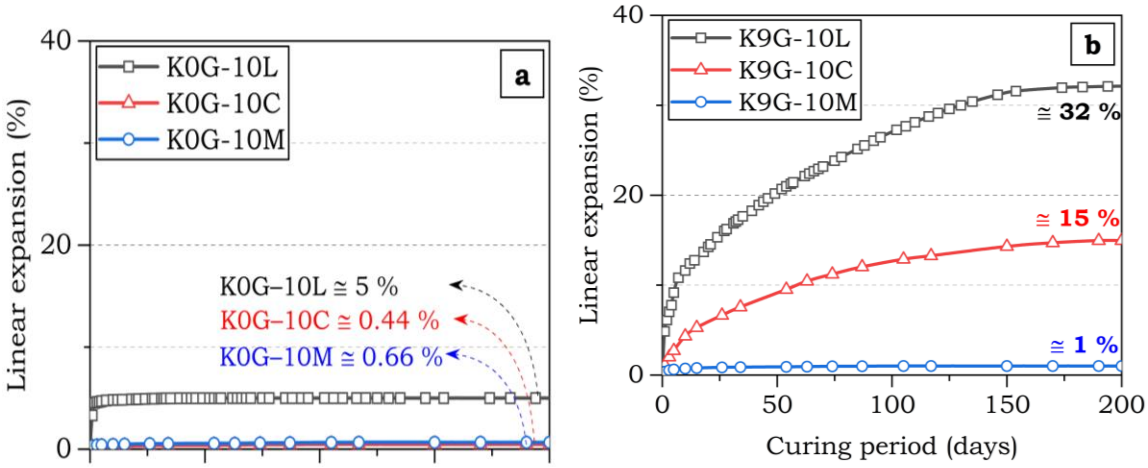

Fig.7: Linear expansion plots of **a)** pure kaolin and **b)** gypseous kaolin specimens, made with cement, lime and magnesium oxide.

The superiority of 10%C on the expanse of 10%L and 10%M in the restriction of expansion is possibly due to the faster hydration process, as it induces higher earlier UCS. The higher strength prevents the reorientation of soil particles and the enlargement of inter-particle pore spacing, of which the latter induces a reduced sorptivity [49]. As for the dominance of 10%M over 10%L, this can be assigned to the fineness of MgO, and the degree of saturation of the stabilized matrix [8]. The extreme fineness of MgO enables homogeneity of MgO distribution and eases the ion migration within the system. This improvement in ion distribution facilitates a proper fabric modification, thus reducing the repulsion force between soil particles and eventually minimizing the water adsorption of soil particles [8,14]. The higher saturation level of K9G-10%M, which is anticipated to be higher than the K9G-10%L because of the exothermic reaction of CaO, is also deemed to be a contributor to the superiority of 10%M over 10%L. This is because the higher saturation degree improves the water pore interconnection within the system [26], thus a homogenous and accelerated ion migration has occurred, and thereby lesser capillary forces are exerted through the rise of water within the stabilized samples.

In the presence of gypsum, the stabilizer domination order, however, was changed, where 10%M yielded the lowest expansion of 1%, relative to that of 15% and 24% experienced by gypseous specimen stabilised with cement (K9G-10%C) and lime (K9G-10%L), respectively. With further in-depth, however, it can be inferred that the negative effect of sulfate was not consistent across all the formations, where lime-based specimens experienced the greatest swelling gain of 27%, representing a swelling gain ratio of about 140% relative to its stabilized none-sulfate counterpart, whereas 10%C- and 10%M-based specimens yielded a swelling gain of 14.5% and 0.4%, respectively. The difference in the swelling trend can be credited to the concentration of ettringite crystals grown during the reaction [30], which was reinforced by the DTG curve (discussed later). These produced minerals grow in pores as a needle or rod-shaped crystals and have a high-water absorption capability [6]. On the continuous growth of ettringite crystalles, internal stress is generated once these minerals intersected with each other or with soil particles, causing cracks and expansion of the stabilized system, and such an expansion is proportional to the amount of ettringite formed.

3- Derivative thermogravimetric analysis

The 7-day derivative thermogravimetric (DTG) of pure kaolin and gypseous kaolin samples made with 10%L, 10%C and 10%M are plotted in **Fig.8**, alongside demonstrative notes for the causativeness of the key peaks.

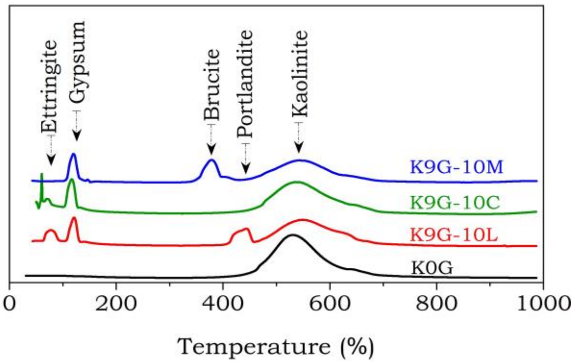

Fig.8: The 7-days DTG curves of pure kaolin and gypseous kaolin samples, made with 10% of cement, lime and magnesium oxide.

On the 7 days of moist curing, the pure kaolin specimen revealed the presence of a major endothermic peak at a temperature of 400-700°C due to the decomposition of kaolinite minerals [37]. On the use of 10%L, 10%C, and 10%M for the stabilization of gypseous kaolin (K9G-10%L), the DTG analysis exhibited four additional peaks; 1) the first peak at 50-100°C owing to the dehydration of ettringite [6]; 2) the second peak at a temperature range of 100-200°C due to the dehydration of moisture content of gypsum crystallization [30]; 3) the third peak at 350-450°C due to the decomposition of brucite [8]; and 4) the fourth peak at 400-500°C due to the decomposition of portlandite [6]. By comparing the height of ettringite peaks, it was apparent that the ettringite mineral was only formed in gypseous kaolin specimens stabilized with a calcium-based stabilizer, and such a mineral was more pronounced in the case of K9G-10%L. This was also confirmed by the higher gypsum peak, both of which are in support of why K9G-10%L yielded a superior UCS gain in the presence of sulfate. Apart from ettringite and gypsum peaks, portlandite and brucite peaks were also detected in K9G-10%L and K9G-10%M, respectively, indicating the incomplete consumption of lime and magnesium oxide through the fabric modification, which in turn indicates the surplus of both binders. This surplus binder content is not favorable, as it prevents the dissolution of soil, delays the pozzolanic reactions, and reduces the cohesion of the system. Therefore, this is in partial support of why lime and magnesium oxide yielded a lower UCS relative to cement, particularly in the absence of sulfate.

Conclusions

The main conclusions of the experimental investigations of this research can be illustrated as follows:

Stabilisation of pure kaolin using Portland cement yielded the highest UCS and lowest linear expansion, relative to both lime and magnesium oxide. This is due to the higher concentration of

Si^{+4} and Al^{+3} ions of Portland cement, which provide the needed oxides for the nucleation and growth of hydrates that are main responsible for the interlocking of the system.

The presence of sulfate (gypsum) in kaolin soil stabilised with calcium-based binders (Lime and Portland cement) yielded an increase in the UCS and linear expansion due to the formation of ettringite, and such an increase was more pronounced in samples stabilized with quicklime.

The utilisation of MgO in the stabilisation of gypsum-dosed kaolin soil experienced the lowest unconfined compressive strength and the lowest linear expansion magnitude due to the restriction of ettringite.

The limitations of the current research study that may have an influence on the generalisation of the experimentation results of this research study, are the use of artificial gypsum-dosed soil, the use of a constant moisture level, and the use of a single source of sulfate (gypsum). Therefore, to enable the generalisation of the outcomes emerged from the laboratory experimentations conducted on the semi-processed industrial soil, research studies concerning the use of different natural soils, different sources of sulfate, and different moisture contents are recommended for future work to overcome this deficiency.

Overall, the use of MgO or cement experienced superior effectiveness in the inhibition of swelling of non-sulfate kaolin, whereas only the MgO demonstrated an accepted swelling in the existence of gypsum. This finding may have some bearing on the current practices, and relevant to all the engineers involved in soil stabilisation and suppression of ettringite-induced expansion, as this document will serve as a helpful resource of in-depth information on soil stabilisation.

References

[1] Al-Atroush, M.E., and Sebaey, T.A., (2021), Stabilization of expansive soil using hydrophobic polyurethane foam: A review., Transportation Geotechnics., **27**, 100494. DOI: 10.1016/j.trgeo.2020.100494.

[2] Ikeagwuani, C.C., and Nwonu, D.C., (2019), Emerging trends in expansive soil stabilisation: A review., Journal of rock mechanics and geotechnical engineering., **11**(2), 423-440. DOI: 10.1016/j.jrmge.2018.08.013.

[3] Kalkan, E., (2011), Impact of wetting–drying cycles on swelling behavior of clayey soils modified by silica fume., Applied clay science., **52**(4), 345-352. DOI: 10.1016/j.clay.2011.03.014.

[4] Jha, A.K., and Sivapullaiah, P.V., (2016), Volume change behavior of lime treated gypseous soil—influence of mineralogy and microstructure., Applied Clay Science., **119**, pp.202-212. DOI: 10.1016/j.clay.2015.09.017.

[5] Cheshomi, A., Eshaghi, A., and Hassanpour, J., (2017), Effect of lime and fly ash on swelling percentage and Atterberg limits of sulfate-bearing clay., Applied Clay Science., **135**, 190-198. DOI: 10.1016/j.clay.2016.09.019.

[6] Ebailila, M., Kinuthia, J., and Oti, J., (2022), Suppression of Sulfate-Induced Expansion with Lime–Silica Fume Blends., Materials., **15**(8), 2821. DOI: 10.3390/ma15082821.

[7] Seco, A., Miqueleiz, L., Prieto, E., Marcelino, S., García, B., and Urmeneta, P., (2017), Sulfate soils stabilization with magnesium-based binders., Applied Clay Science., **135**, 457-464. DOI: 10.1016/j.clay.2016.10.033.

[8] M. Ebailila, Sulfate soil stabilisation with silica fume-based binders, Doctoral Thesis, University of South Wales, England, UK, 2022.

[9] Yi, Y., Liska, M., and Al-Tabbaa, A., (2014), Properties of two model soils stabilized with different blends and contents of GGBS, MgO, lime, and PC., Journal of Materials in Civil Engineering., **26**(2), 267-274. DOI: 10.1061/(ASCE)MT.1943-5533.0000806.

[10] Jin, F., and Al-Tabbaa, A., (2014), Evaluation of novel reactive MgO activated slag binder for the immobilisation of lead and zinc., Chemosphere., **117**, 285-294. DOI: 10.1016/j.chemosphere.2014.07.027.

[11] Li, W., Ni, P., and Yi, Y., (2019), Comparison of reactive magnesia, quick lime, and ordinary Portland cement for stabilization/solidification of heavy metal-contaminated soils., Science of the Total Environment., **671**, 741-753. DOI: 10.1016/j.scitotenv.2019.03.270.

[12] Yi, Y., Zheng, X., Liu, S. and Al-Tabbaa, A., (2015), Comparison of reactive magnesia-and carbide slag-activated ground granulated blastfurnace slag and Portland cement for stabilisation of a natural soil., Applied Clay Science., **111**, 21-26. DOI: 10.1016/j.clay.2015.03.023.

[13] Liska, M., and Al-Tabbaa, A., (2009), November. Ultra-green construction: reactive magnesia masonry products., In Proceedings of the Institution of Civil Engineers-Waste and Resource Management., **162**, 185-196. DOI: 10.1680/warm.2009.162.4.185.

[14] Ebailila, M., Kinuthia, J., Oti, J., and Al-Waked, Q., (2022), Sulfate soil stabilisation with binary blends of lime–silica fume and lime–ground granulated blast furnace slag., Transportation Geotechnics., **37**, 100888. DOI: 10.1016/j.trgeo.2022.100888.

[15] Seco, A., Ramírez, F., Miqueleiz, L., and García, B., (2011), Stabilization of expansive soils for use in construction., Applied Clay Science., **51**(3), 348-352. DOI: 10.1016/j.clay.2010.12.027.

[16] Li, W., Yi, Y., and Puppala, A.J., (2020), Suppressing ettringite-induced swelling of gypseous soil by using magnesia-activated ground granulated blast-furnace slag., Journal of Geotechnical and Geoenvironmental Engineering., **146**(7), 06020008. DOI: 10.1061/(asce)gt.1943-5606.0002292.

[17] Yi, Y., Gu, L., Liu, S., and Jin, F., (2016), Magnesia reactivity on activating efficacy for ground granulated blastfurnace slag for soft clay stabilisation. Applied Clay Science., **126**, 57-62. DOI: 10.1016/j.clay.2016.02.033.

[18] Yi, Y., Li, C., Liu, S., and Al-Tabbaa, A., (2014), Resistance of MgO–GGBS and CS–GGBS stabilised marine soft clays to sodium sulfate attack., Géotechnique., **64**(8), 673-679. DOI: 10.1680/geot.14.t.012.

[19] Yi, Y., Liska, M., Unluer, C., and Al-Tabbaa, A., (2013), Carbonating magnesia for soil stabilization., Canadian Geotechnical Journal., **50**(8), 899-905. DOI: 10.1139/cgj-2012-0364.

[20] Yi, Y., Liska, M., Jin, F., and Al-tabbaa, A., (2016), Mechanism of reactive magnesia-GGBS soil stabilisation., Canadian Geotechnical Journal., **55**, 773–782. DOI: 10.1139/cgj-2015-0183.

[21] Yi, Y., Gu, L., and Liu, S., (2015), Microstructural and mechanical properties of marine soft clay stabilized by lime-activated ground granulated blastfurnace slag., Applied Clay Science., **103**, 71-76. DOI: 10.1016/j.clay.2014.11.005.

[22] Yi, Y., Liska, M., and Al-Tabbaa, A., (2012) Initial investigation into the use of GGBS-MgO in soil stabilisation., In Grouting and Deep Mixing 2012., 444-453.

[23] Goodarzi, A.R., and Movahedrad, M., (2017), Stabilization/solidification of zinc-contaminated kaolin clay using ground granulated blast-furnace slag and different types of activators., Applied Geochemistry., **81**, 155-165. DOI: 10.1016/j.apgeochem.2017.04.014.

[24] Gu, K., Jin, F., Al-Tabbaa, A., Shi, B., Liu, C., and Gao, L., (2015), Incorporation of reactive magnesia and quicklime in sustainable binders for soil stabilisation., Engineering Geology., **195**, 53-62. DOI: 10.1016/j.enggeo.2015.05.025.

[25] BS EN 197-1:2011, Cement — Part 1: Composition, specifications and conformity criteria for common cements, BSI Standards Limited, London, UK, 2011. https://doi.org/10.3403/30205527.

[26] Beetham, P., Dijkstra, T., Dixon, N., Fleming, P., Hutchison, R., and Bateman, J., (2015), Lime stabilisation for earthworks: a UK perspective., Proceedings of the Institution of Civil Engineers-Ground Improvement., **168**(2), 81-95. DOI: 10.1680/grim.13.00030.

[27] Boardman, D.I., Glendinning, S., and Rogers, C.D.F., (2001), Development of stabilisation and solidification in lime–clay mixes., Geotechnique., **51**(6), 533-543. DOI: 10.1680/geot.2001.51.6.533.

[28] Obuzor, G.N., Kinuthia, J.M., and Robinson, R.B., (2011), Enhancing the durability of flooded low-capacity soils by utilizing lime-activated ground granulated blastfurnace slag (GGBS)., Engineering Geology., **123**(3), 179-186. DOI: 10.1016/j.enggeo.2011.07.009.

[29] Afrin, H., (2017), A review on different types soil stabilization techniques., International Journal of Transportation Engineering and Technology., **3**(2), 19-24. DOI: 10.11648/j.ijtet.20170302.12.

[30] Ebailila, M., Kinuthia, J., and Oti, J., (2022), Role of Gypsum Content on the Long-Term Performance of Lime-Stabilised Soil., Materials., **15**(15), 5099. DOI: 10.3390/ma15155099.

[31] BS EN ISO 17892-7: 2018, Geotechnical investigation and testing-Laboratory testing of soil — Part 7: Unconfined compression test, BSI Standards Limited, London, UK, 2018.

[32] BS EN 13286-49: 2004, Unbound and hydraulically bound mixtures — Part 49: Accelerated swelling test for soil treated by lime and/or hydraulic binder, BSI Standards Limited, London, UK, 2004.

[33] Obuzor, G.N., Kinuthia, J.M., and Robinson, R.B., (2011), Utilisation of lime activated GGBS to reduce the deleterious effect of flooding on stabilised road structural materials: A laboratory simulation., Engineering geology., **122**(3-4), 334-338. DOI: 10.1016/j.enggeo.2011.06.010.

[34] Oti, J.E., Kinuthia, J.M., and Robinson, R.B., (2014), The development of unfired clay building material using Brick Dust Waste and Mercia mudstone clay., Applied clay science., **102**, 148-154. DOI: 10.1016/j.clay.2014.09.031.

[35] Kinuthia, J.M., and Nidzam, R.M., (2011), Towards zero industrial waste: Utilisation of brick dust waste in sustainable construction., Waste Management., **31**(8), 1867-1878. DOI: 10.1016/j.wasman.2011.03.020.

[36] Behnood, A., (2018), Soil and clay stabilization with calcium-and non-calcium-based additives: A state-of-the-art review of challenges, approaches and techniques., Transportation Geotechnics., **17**, 14-32. DOI: 10.1016/j.trgeo.2018.08.002.

[37] Al-Mukhtar, M., Lasledj, A., and Alcover, J.F., (2014), Lime consumption of different clayey soils., Applied Clay Science., **95**, 133-145. DOI: 10.1016/j.clay.2014.03.024.

[38] Sharma, L.K., Sirdesai, N.N., Sharma, K.M., and Singh, T.N., (2018), Experimental study to examine the independent roles of lime and cement on the stabilization of a mountain soil: A comparative study., Applied Clay Science., **152**, 183-195. DOI: 10.1016/j.clay.2017.11.012.

[39] Degirmenci, N., Okucu, A., and Turabi, A., (2007), Application of phosphogypsum in soil stabilization., Building and environment., **42**(9), 3393-3398. DOI: 10.1016/j.buildenv.2006.08.010.

[40] Konan, K.L., Peyratout, C., Smith, A., Bonnet, J.P., Rossignol, S., and Oyetola, S., (2009), Comparison of surface properties between kaolin and metakaolin in concentrated lime solutions., Journal of colloid and interface science., **339**(1), 103-109. DOI: 10.1016/j.jcis.2009.07.019.

[41] Choobbasti, A.J., and Kutanaei, S.S., (2017), Microstructure characteristics of cement-stabilized sandy soil using nanosilica., Journal of Rock Mechanics and Geotechnical Engineering., **9**(5), 981-988. DOI: 10.1016/j.jrmge.2017.03.015.

[42] Puppala, A.J., Talluri, N., and Chittoori, B.C., (2014), Calcium-based stabiliser treatment of sulfate-bearing soils., Proceedings of the Institution of Civil Engineers-Ground Improvement., **167**(3), 162-172. DOI: 10.1680/grim.13.00008.

[43] Jha, A.K., and Sivapullaiah, P.V., (2014), Role of gypsum on microstructure and strength of soil., Environmental Geotechnics., **3**(2), 78-89. DOI: 10.1680/envgeo.13.00084.

[44] Aldaood, A., Bouasker, M. and Al-Mukhtar, M., (2016), Effect of water during freeze–thaw cycles on the performance and durability of lime-treated gypseous soil., Cold Regions Science and Technology., **123**, 155-163. DOI: 10.1016/j.coldregions.2015.12.008.

[45] Aldaood, A., Bouasker, M., and Al-Mukhtar, M., (2021), Mechanical behavior of gypseous soil treated with lime., Geotechnical and Geological Engineering, **39**, 719-733. DOI: 10.1007/s10706-020-01517-w.

[46] Aldaood, A., Bouasker, M., and Al-Mukhtar, M., (2014), Free swell potential of lime-treated gypseous soil., Applied Clay Science., **102**, 93-103. DOI: 10.1016/j.clay.2014.10.015.

[47] Aldaood, A., Bouasker, M., and Al-Mukhtar, M., (2014), Geotechnical properties of lime-treated gypseous soils., Applied Clay Science., **88**, 39-48. DOI: 10.1016/j.clay.2013.12.015.

[48] Yi, Y., Zheng, X., Liu, S., and Al-Tabbaa, A., (2015), Comparison of reactive magnesia-and carbide slag-activated ground granulated blastfurnace slag and Portland cement for stabilisation of a natural soil., Applied Clay Science., **111**, 21-26. DOI: 10.1016/j.clay.2015.03.023.

[49] Hossain, K.M.A., Lachemi, M., and Easa, S., (2007), Stabilized soils for construction applications incorporating natural resources of Papua New Guinea., Resources, Conservation and Recycling., **51**(4), 711-731. DOI: 10.1016/j.resconrec.2006.12.003.